Stabilization of Radical Intermediates by an Active-Site Tyrosine Residue in Methylmalonyl-CoA Mutase[†,‡]

Nicolas H. Thomä,[§] Thomas W. Meier,[§,||] Philip R. Evans,[⊥] and Peter F. Leadlay*[,§]

Department of Biochemistry and Cambridge Centre for Molecular Recognition, University of Cambridge, Tennis Court Road, Cambridge, CB2 1GA United Kingdom, and Medical Research Council Laboratory of Molecular Biology, MRC Centre, Hills Road, Cambridge, CB2 2QH United Kingdom

Received June 10, 1998; Revised Manuscript Received August 10, 1998

ABSTRACT: The adenosylcobalamin-dependent methylmalonyl-CoA mutase catalyzes the reversible rearrangement of methylmalonyl-CoA into succinyl-CoA by a free-radical mechanism. The recently solved X-ray crystal structure of methylmalonyl-CoA mutase from *Propionibacterium shermanii* has shown that tyrosine 89 is an active-site residue involved in substrate binding. The role of tyrosine 89, a conserved residue among methylmalonyl-CoA mutases, has been investigated by using site-directed mutagenesis to replace this residue with phenylalanine. The crystal structure of the Tyr89Phe mutant was determined to 2.2 Å resolution and was found to be essentially superimposable on that of wild-type. Mutant and wild-type enzyme have very similar K_M values, but k_{cat} for the Tyr89Phe mutant is 580-fold lower than for wild-type. The rate of release of tritium from 5′-[^{3}H]adenosylcobalamin during the enzymatic reaction and its rate of appearance in substrate and product were measured. The tritium released was found to partition unequally between methylmalonyl-CoA and succinyl-CoA, in a ratio of 40:60 when the reaction was initiated by addition of methylmalonyl-CoA and in a ratio of 10:90 when the reaction was initiated by addition of succinyl-CoA. The overall release of tritium was four times faster when succinyl-CoA was used as substrate. The tritium isotope effect on the enzyme catalyzed hydrogen transfer, measured with methylmalonyl-CoA as a substrate, was $k_H/k_T = 30$, which is within the expected range for a full primary kinetic tritium isotope effect. The different partitioning of tritium, dependent upon which substrate was used, and the normal value for the kinetic tritium isotope effect contrast markedly with the behavior of wild-type mutase. It appears that the loss of a single interaction involving the hydroxyl group of tyrosine 89 both affects the stability of radical intermediates and decreases the rate of interconversion of the substrate- and product-derived radicals.

Methylmalonyl-CoA[1] mutase catalyzes the reversible isomerization of (2R)-methylmalonyl-CoA and succinyl-CoA (*1*, *2*). The protein belongs to a group of AdoCbl-dependent enzymes catalyzing unusual 1,2-rearrangements and is the only one found in both bacterial and animal cells (for reviews, see refs *3*−*5*). The rearrangement of methylmalonyl-CoA to succinyl-CoA follows the general reaction course of AdoCbl-dependent enzymes (Figure 1). The first step in the mutase-catalyzed reaction is the homolytic cleavage of the Co−C bond of the cofactor to generate a cob(II)alamin radical and a carbon-centered deoxyadenosyl radical (*6*−*9*). In a closely linked step which may possibly be concerted with cobalt−carbon bond cleavage (*10*), the deoxyadenosyl radical abstracts a hydrogen atom from the methyl group of methylmalonyl-CoA (I, see Figure 1) to generate a primary radical (II). The latter then rearranges by an unknown mechanism to the secondary radical of succinyl-CoA (III). Reabstraction of a hydrogen from the

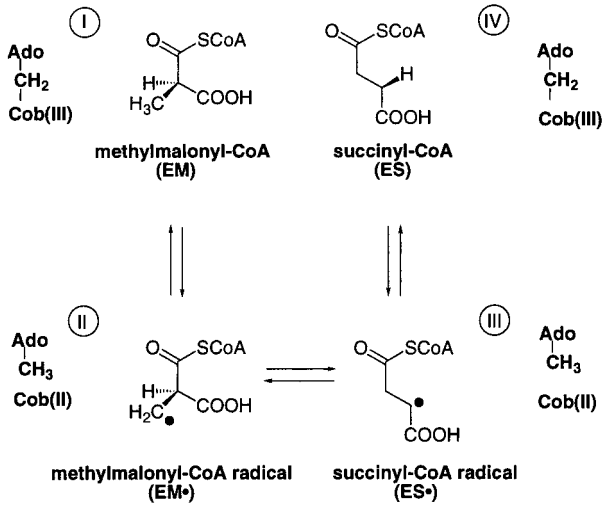

FIGURE 1: Mechanistic scheme for the mutase-catalyzed rearrangement.

[†]This work was supported by the Medical Research Council, U.K. (G8806378CB).

[‡] The Protein Data Bank (PDB) accession code for the atomic coordinates of the Tyr89Phe mutant of methylmalonyl-CoA mutase is 5req.

* Author to whom correspondence should be addressed. Tel: + 44-1223-33656. Fax: +44-1223-333656.

[§] University of Cambridge.

[||] Current Address: Cilag Analytical R&D, Hochstrasse 201, 8265 Schaffhausen, Switzerland.

[⊥] MRC Centre.

[1] Abbreviations: AdoCbl, adenosylcobalamin or coenzyme-B_{12}; CoA, coenzyme A; TFA, trifluoroacetic acid; Tyr89, tyrosine A89 of the mutase α-subunit; Arg207, arginine A207 of the mutase α-subunit; His244, histidine A244 of the mutase α-subunit.

S0006-2960(98)01375-0 CCC: $15.00
Published on Web 09/23/1998

cofactor, to give the product succinyl-CoA (IV) and reform AdoCbl, completes the reaction cycle. The involvement of AdoCbl as the hydrogen acceptor and hydrogen donor in AdoCbl-dependent reactions has been previously demonstrated by several groups in experiments using tritium-labeled substrate and tritium-labeled cofactor (*11*−*13*).

At least three specific roles have been mooted for the protein in the AdoCbl-dependent skeletal rearrangement catalyzed by methylmalonyl-CoA mutase: first, and most obviously, the remarkable enhancement of the homolytic cleavage of the carbon−cobalt bond of the enzyme-bound AdoCbl, by an estimated 10^{10}−10^{11}-fold (*10*, *14*, *15*) compared to free AdoCbl; second, the effective protection of the free-radical intermediates; and third, direct catalysis of the rearrangement step itself. The recent determination of the X-ray crystal structure of the methylmalonyl-CoA mutase from *P. shermanii*, both in the presence (*16*) and in the absence (*17*) of substrates or substrate analogues, has provided clear evidence that the binding of CoA ester substrates involves a major conformational change in which the binding energy is apparently used to drive the closure of the active site and the displacement of the adenosyl group from the corrin. As in the methylcobalamin-dependent methionine synthase (*18*, *19*), the other axial ligand is provided by a histidine residue hydrogen bonded to an aspartic acid (*16*), but there is an unprecedentedly long Co−N bond in the mutase-bound AdoCbl, which may additionally contribute to the labilization of the axial Co−C bond (*16*). The crystal structure of the mutase also provided support for a role of the enzyme, in the protection of radical intermediates during the rearrangement. The conformational change upon substrate binding creates a sealed and deeply buried active-site environment shielding intermediates from solvent.

Little information, however, is available concerning the extent to which active-site amino acids are directly involved in catalysis of the radical rearrangement, rather than providing a chemically inert environment (*20*). The crystal structure of methylmalonyl-CoA mutase revealed that only a few polar active-site amino acids, in particular histidine 244, arginine 207, and tyrosine 89, are in direct contact with the substrate (*16*).

We focused on tyrosine 89 since tyrosine-based protein radicals have been found to play an important role in catalysis by a number of radical enzymes including ribonucleotide reductase, prostaglandin H synthase, cytochrome *c* oxidase, and photosystem II (for review, see refs *21* and *22*). To investigate its role in catalysis by methylmalonyl-CoA mutase, we have substituted tyrosine 89, which is a wholly conserved residue in methylmalonyl-CoA mutases, from various sources. The mutant Tyr89Phe was characterized in several ways: first, by determination of its crystal structure; second, by determination of its steady-state parameters; third, by measurement of kinetic deuterium isotope effects; and finally, by studying the rate of tritium release, under various conditions, from 5′-[^{3}H]adenosylcobalamin bound to the mutant enzyme. The structural effects of the mutant were found to be entirely localized to the active site, and the effects found on catalysis are consistent with tyrosine 89 playing a key role in both the stabilization of free-radical intermediates and the enhancement of their rates of interconversion.

MATERIALS AND METHODS

Materials. The purification of methylmalonyl-CoA mutase from recombinant *Escherichia coli* strains has been described previously (*23*), and the Tyr89Phe mutant protein behaved identically to the wild-type during purification. Radiolabeled 5′-[^{3}H]AdoCbl with a specific activity of 12 000 dpm/nmol was added to the Tyr89Phe mutant apoenzyme before the final purification step, and Tyr89Phe mutant methylmalonyl-CoA mutase was eluted as holoenzyme. Enzymic synthesis and purification of 5′-[^{3}H]AdoCbl was done as described by Marsh (*24*). The synthesis of [$^2H_4$]-succinyl-CoA was as described by Simon and Shemin (*25*). Succinylcarbadethia-coenzyme A (*26*) was synthesized as described previously (*7*). All other chemicals were purchased from commercial suppliers and used without further purification.

Construction of the Tyr89Phe Mutant. Tyrosine 89 on the α-subunit of methylmalonyl-CoA mutase, the structural gene for which is designated *mutB*, was mutated to phenylalanine using a PCR-based mega-priming approach (*27*). PCR was performed on a Robocycler 40 (Stratagene) using *Pfu* polymerase (Stratagene). A 2.3 kb *Bst*EII fragment was identified as the smallest unique restriction fragment in the expression plasmid pMEX2 (*23*) that harbored the codon for tyrosine 89. First, a 300 bp PCR fragment extending from the 5′-end of the *Bst*EII fragment (5′-CTG CTC CTC GGC GGT CAC CAC ATA-3′) to the desired mutation on the 3′-end (5′-ATT CGC CAG TTC GCC GTt TCT CCA-3′) was generated using the two primers (100 pmol), plasmid pMEX2 (100 ng), dNTPs (250 nmol), and 5U *Pfu* DNA polymerase in a total volume of 100 μL and 25 cycles each of 95 °C for 45 s, 50 °C for 30 s, and then 72 °C for 150 s, including a hot start. The mutagenic *Bst*EII fragment was assembled using primer 5′-CCC GAA GAA GCT TGG TTA CCC CGG CG-3′ (100 pmol) comprising the 3′-end of the *Bst*EII fragment and the megapriming fragment (100 pmol) comprising the 5′-end of the *Bst*EII fragment. The cycling was initiated using a long first annealing cycle (95 °C for 0.45 s, 48 for 150 s and 72 °C for 180 s) including a hot start. This was followed by 24 cycles of 95 °C for 45 s, 51 °C for 50 s, and 72 °C for 150 s. The reactions were carried out in the presence of 10% dimethyl sulfoxide. The mutant *Bst*EII fragment was completely sequenced to confirm that only the desired mutation had occurred and was subsequently subcloned into pMEX-2 to obtain plasmid pMEX-Y89F.

Crystallization of the Tyr89Phe Mutant. Crystals of the complex between the Tyr89Phe holomutase and the alternative substrate succinylcarbadethia-CoA were grown by vapor diffusion at 23 °C. A 10 μL hanging drop consisting of equal volumes of reservoir and protein solution was equilibrated against the reservoir solution. The protein solution consisted of 20 mg/mL mutase protein, 100 μM AdoCbl, 4 mM succinylcarbadethia-CoA, 14% w/v poly(ethylene glycol) 4000, and 20% v/v glycerol in 100 mM Tris-HCl buffer, pH 7.5; the reservoir solution 14% w/v poly(ethylene glycol) 4000 and 20% v/v glycerol in 100 mM Tris-HCl buffer, pH 7.5. The crystal used for data collection was monoclinic, spacegroup $P2_1$ with cell parameters $a = 120.2$ Å, $b = 161.9$ Å, $c = 88.7$ Å, and $\beta = 104.9°$.

Data Collection, Structure Determination, and Refinement. A 98% complete data set to 2.2 Å resolution consisting of 171 783 unique reflections was collected on the X-ray diffraction beamline at Elettra, Trieste, Italy, at a wavelength of 1.24 Å (10 keV). The crystal was suspended directly from the hanging drop in a thin film of liquid and frozen at 95K in the cold stream with a 600 Series Cryostream Cooler (Oxford Cryosystems, Oxford, U.K.) and kept in the dark during the data collection. Data were collected in two passes with different exposure times with a 180 mm diameter MAR research image plate (Hamburg, Germany) and integrated with MOSFLM. Scaling and processing were performed using the CCP4 suite programs (Collaborative Computational Project, No. 4, 1994); data was merged with R_{merge} of 0.05 with multiplicity 3.3, I/σ 13.4 (2.2 in the outer shell, 2.3 to 2.2 Å); and the *B*-factor derived from the Wilson plot was 38 Å^2. The structure was solved by molecular replacement using one $\alpha\beta$ heterodimer from a previously determined structure of an inhibitor complex with 3-carboxypropyl-CoA (P. R. Evans, unpublished material). Calculations were carried out at 4 Å resolution using the program AMoRe (*28*). Two heterodimeric molecules were found in the asymmetric unit, in a very similar arrangement to that seen in the desulfo-CoA complex (*16*). The molecular replacement solution after rigid body refinement at 4 Å resolution had a correlation coefficient of 78.7% and an *R*-factor of 29%. The model was refined using REFMAC (*29*) and rebuilt using the program O (*30*). Noncrystallographic symmetry restraints were applied to keep the two molecules in the asymmetric unit in a similar conformation. The model has an *R*-factor of 25% for 95% of the data to 2.2 Å resolution, with an R_{free} for the remaining 5% of 29.8%.

UV/Vis Spectrophotometry. UV/vis spectra were measured at 30 °C in 50 mM Tris-HCl buffer, pH 7.5, using a Varian Cary 1E spectrophotometer. Enzyme concentration was determined assuming 1 mol of bound AdoCbl/heterodimer, and extinction coefficients for bound AdoCbl ϵ(525 nm) = 8000 cm^{-1} M^{-1}, ϵ(336 nm) = 11 000 cm^{-1} M^{-1}, and ϵ(376 nm) = 12 800 cm^{-1} M^{-1} (*31*).

Steady-State Kinetic Measurements. Methylmalonyl-CoA mutase was assayed using a coupled enzyme spectrophotometric assay (*32*, *33*). The steady-state kinetic parameters K_M and k_{cat} for wild-type enzyme and for Tyr89Phe mutant were determined by measuring initial velocities at various concentrations of succinyl-CoA and fitting the data to linear Hanes plots of s against s/v (reviewed in ref *34*). The deuterium isotope effect on V_{max} was measured under noncompetitive conditions using an initial substrate concentration of 2 mM for both succinyl-CoA and [$^2H_4$]succinyl-CoA.

HPLC-Based Assay for Methylmalonyl-CoA Mutase Turnover. To a solution of 1.8 mM Tyr89Phe mutant enzyme containing [^{3}H]AdoCbl (12 000 dpm/nmol) in 50 mM Tris-HCl, pH 7.5, at 30 °C, was added CoA-ester substrate to a final concentration of 1 mM. Samples (100 μL) were withdrawn after various periods of time and quenched by addition of 100 mL of 0.5% trifluoracetic acid. The samples were immediately frozen on dry ice and stored at −20 °C before HPLC analysis. All reactions were carried out in black Eppendorf tubes to avoid photolysis of the cobalamin.

HPLC Analysis of Radiolabeled Substrates and Products. Methylmalonyl-CoA, succinyl-CoA, and AdoCbl were separated at 10 °C by HPLC on a reversed-phase column (Pharmacia μRPC C2/C18, 2.1 × 100 mm) attached to a SMART system (Pharmacia). Samples of 100 μL were injected onto the column, which had been preequilibrated with 100 mM phosphate buffer, pH 5.0, and the compounds were eluted with a linear gradient of increasing methanol concentration. Methylmalonyl-CoA eluted at 34%, succinyl-CoA at 36%, and AdoCbl at 50% methanol. The flow rate was 100 μL/min, and compounds were detected by monitoring the absorbance simultaneously at 256, 280, and 520 nm. The simultaneous measurement at 256, 280, and 520 nm allowed the turnover to be calculated directly from the UV trace at 280 nm, and avoided the need for ^{14}C-labeled substrate. The recovery of radiolabeled substrates was determined with standard samples and found to be >95%.

Scintillation Counting. Scintillation counting was done on a Beckman LS3801 instrument using OptiPhase HiSafe scintillation liquid. Pooled fractions of methylmalonyl-CoA, succinyl-CoA, and AdoCbl were counted for tritium. A quench curve was established, and commercially available standards were used to correct for quenching of the samples.

Data Calculation. To correct for pipetting errors, total radioactivity of methylmalonyl-CoA, succinyl-CoA, and AdoCbl was normalized. The data were plotted and curves fitted using the KaleidaGraph program (Abelbeck Software).

RESULTS

Purification of the Tyr89Phe Mutant of Methylmalonyl-CoA Mutase. The mutant enzyme was purified to homogeneity from cell extracts of recombinant *Escherichia coli*, essentially as described for wild-type enzyme (*23*). The mutant bound 1 mol of AdoCbl/mole of enzyme and its UV−vis absorption spectrum was identical to that of the wild-type enzyme (data not shown).

Determination of the Crystal Structure of the Tyr89Phe Mutant. The Tyr89Phe mutant cocrystallized in the presence of the nonhydrolyzable alternative substrate succinylcarbadethia-CoA under conditions identical to those used for wild-type (*35*). A section of the electron density map around the active site is shown in Figure 2. Superimposition of the wild-type and mutant structures showed that the active sites of the two structures are essentially identical (backbone rms = 0.02 Å) within experimental error. In the mutant structure, the hydroxyl group of the original tyrosine 89 is clearly absent and there is no water molecule in its place. However, the electron density of the aromatic ring of phenylalanine 89 is slightly broadened indicative of a small increase in mobility (Figure 2). The substrate density was modeled as an equimolar mixture of succinylcarbadethia-CoA and (2*R*)-methylmalonycarbadethia-CoA. The conformation and the position of the methylmalonyl and succinyl moieties of the respective substrates were found to be identical with the wild-type, within experimental error. As observed for previous structures with bound substrate analogues (*16*, *35*), there was no observable density that could safely be ascribed to the 5′-deoxyadenosyl group. The corrin appears as a 5-coordinated cobalt(II) species (*16*).

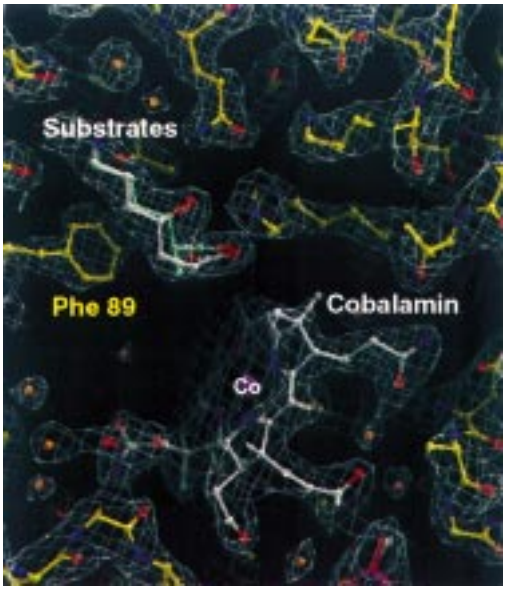

FIGURE 2: Section of the $2F_{obs} - F_{calc}$ SIGMAA weighted electron density map of the active site of Tyr89Phe methylmalonyl-CoA mutase containing bound substrates at 2.2 Å. Methylmalonylcarbadethia-CoA is shown in green while succinylcarbadethia-CoA is shown in white.

Table 1. Steady-State Kinetic Parameters of Mutase Wild-Type and Tyr89Phe Mutant

	K_M (μM)	k_{cat} (s^{-1})	k_{cat}/K_M ($s^{-1}M^{-1}$)	V_H/V_D
mutase wild-type	96 ± 0.5	48 ± 0.5	500	3.4 ± 0.5
Tyr89Phe mutant	64 ± 2.0	0.081 ± 0.01	1.3	5.2 ± 0.8

Steady-State Kinetic Analysis. Steady-state kinetic parameters for wild-type and mutant enzymes were determined for the substrate succinyl-CoA using a coupled enzyme spectrophotometric assay. Initial rates (v) at various substrate concentrations (s) were measured for both enzymes and fitted to plots of s against s/v (*34*). The derived values for K_M and k_{cat} are shown in Table 1. The values obtained for the wild-type enzyme were in good agreement with previously measured values (*32*). Comparison of mutant with wild-type showed that the specific tyrosine to phenylalanine mutation does not significantly affect K_M, but k_{cat} is lowered about 580-fold.

Deuterium Isotope Effect. The primary kinetic deuterium isotope effect on conversion of succinyl-CoA into methylmalonyl-CoA was measured using a range of concentrations of, separately, succinyl-CoA, and [$^2H_4$]succinyl-CoA. Isotope effects on V_{max} were obtained from plots of s against s/v (data not shown) (reviewed in ref *34*). The results (Table 1) show a significantly higher kinetic deuterium isotope effect ($k_H/k_D = 5.2 \pm 0.8$) for the mutant enzyme compared to the wild-type ($k_H/k_D = 3.4 \pm 0.5$). The isotope effect measured for the wild-type enzyme was in good agreement with the isotope effect of $k_H/k_D = 3.5$ measured previously by Wölfle et al. (*36*).

Partitioning of Tritium. In general, the experimental arrangement used to study tritium release from [^{3}H]AdoCbl bound to the Tyr89Phe mutant was the same as previously described for wild-type enzyme (*37*). The pathways for migration of tritium during the course of the rearrangement are shown in Figure 3. The results of tritium partitioning

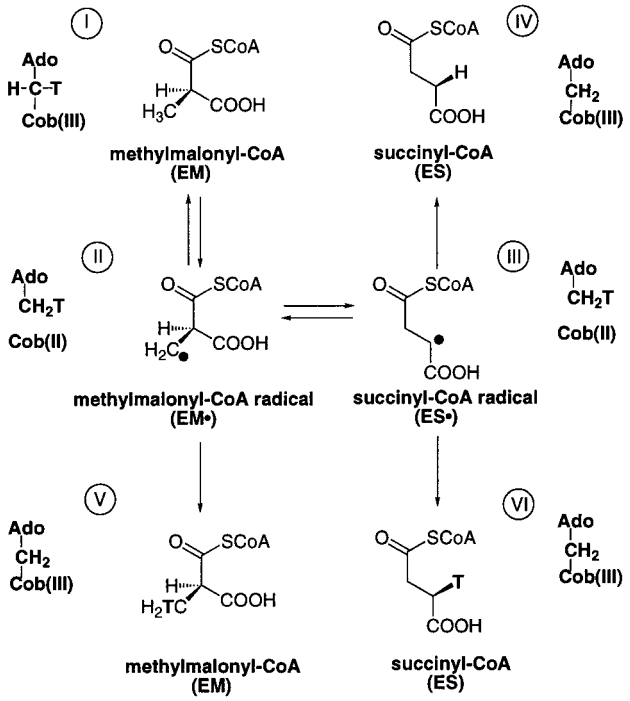

FIGURE 3: Release of tritium from AdoCbl during the rearrangement of methylmalonyl-CoA into succinyl-CoA. Methylmalonyl-CoA binds reversibly to methylmalonyl-CoA mutase (I → II and II → I). The methylmalonyl-CoA radical (II) either abstracts tritium from the cofactor to yield [^{3}H]methylmalonyl-CoA (V) or rearranges to the succinyl-CoA radical (III). The succinyl-CoA radical can then abstract either hydrogen or tritium from AdoCbl to give [^{3}H]-succinyl-CoA (IV) or succinyl-CoA (VI), respectively. Steps III → VI and III → IV are shown as irreversible because under the conditions used the back reaction can be neglected.

when methylmalonyl-CoA was used as a substrate are as shown in Figure 4A. Tritium was released from AdoCbl with a first-order rate constant of $k_{TM} = 0.003\,78\ s^{-1}$. The distribution of tritium between the two CoA-esters was 40:60 in favor of succinyl-CoA, and this ratio did not change within the first 240 s of the reaction. The experiment was repeated using succinyl-CoA as a substrate, and the results were as shown in Figure 4B. Tritium was released from AdoCbl with a first-order rate constant of $k_{TS} = 0.0133\ s^{-1}$, that is, about four times faster than when methylmalonyl-CoA is the substrate. In this experiment, the distribution of the released tritium was 90:10 in favor of succinyl-CoA over methylmalonyl-CoA. This ratio also remained constant within the first 240 ms.

Tritium Isotope Effect. The conversion of methylmalonyl-CoA into succinyl-CoA by the Tyr89Phe mutant enzyme was monitored by integrating the respective areas under the peaks of absorbance for each CoA ester (at 280 nm) after HPLC separation. Turnover was linear for the first 240 s and the calculated turnover number for the mutant enzyme was $k_H = 0.133\ s^{-1}$ (Figure 4C). From the partitioning experiments shown in Figure 5A, it is clear that only 60% of the tritium released from the AdoCbl coenzyme goes into the product succinyl-CoA. The release of tritium in the forward direction was therefore calculated as $k_T = 0.6k_{TM} = 0.0023\ s^{-1}$. Assuming a rapid rotation of the methyl group of enzyme-bound deoxyadenosine (*38*), a statistical factor of 2 had to be taken into consideration. The calculated isotope effect is therefore $k_H/(2k_T) = 30$.

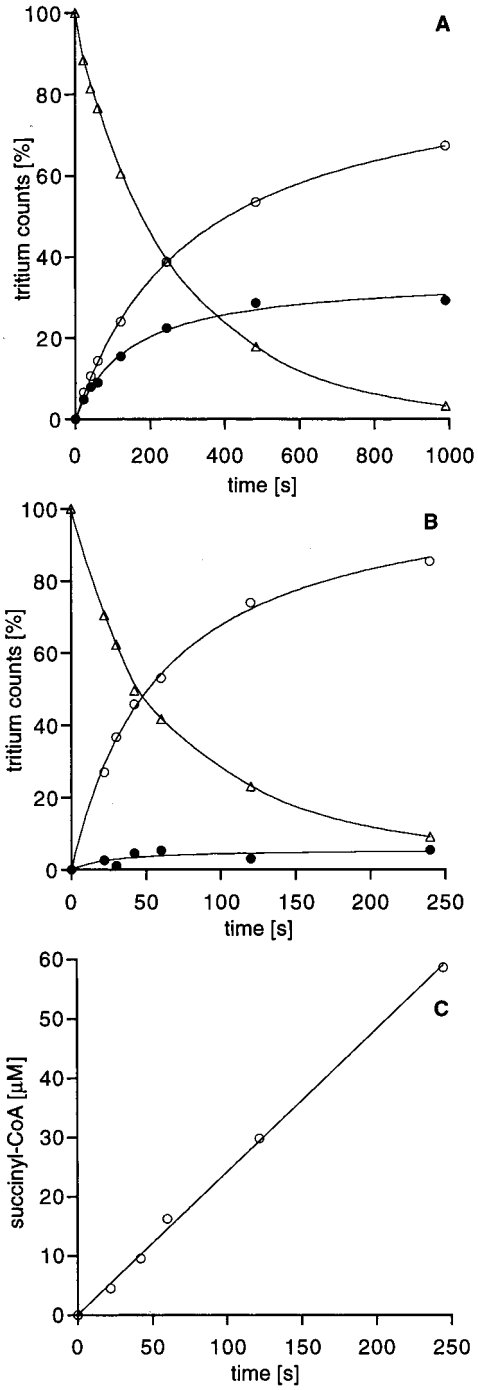

FIGURE 4: (A) Tritium release from AdoCbl (△) and tritium appearance in methylmalonyl-CoA (●) and in succinyl-CoA (○) when methylmalonyl-CoA was added as substrate. (B) As for panel A but succinyl-CoA added as substrate. (C) Formation of succinyl-CoA from methylmalonyl-CoA. Production of succinyl-CoA remained linear for the first 240 s.

DISCUSSION

The mutant enzyme produced by specific substitution of tyrosine 89 in methylmalonyl-CoA mutase by phenylalanine could be purified to homogeneity by the same method as used for wild-type, demonstrating that it retains high affinity for AdoCbl. The X-ray crystal structure of the mutant protein, determined to 2.2 Å resolution, was found to be essentially superimposable on that of wild-type, so that the observed functional differences between mutant and wild-type can be ascribed with reasonable confidence to the effects

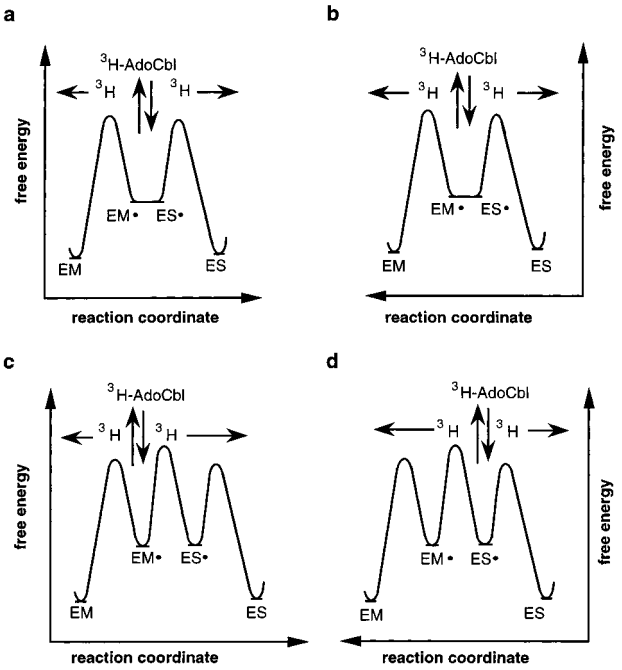

FIGURE 5: Alternative free energy profile for tritium release from adenosylcobalamin. (a) ES• and EM• in rapid equilibrium. Reaction initiated by addition of methylmalonyl-CoA (M). (b) As for panel a but reaction initiated by addition of succinyl-CoA (S). The partitioning of released tritium between M and S will be identical in panels a and b. (c) EM• and ES• interconversion slow. Reaction initiated by addition of methylmalonyl-CoA (M). (d) As for panel c but reaction initiated by addition of succinyl-CoA (S). The partitioning of released tritium between S and M will be different in panels c and d.

of the loss of the phenolic hydroxyl group. The Tyr89Phe mutant remains catalytically active, showing that this residue is not absolutely essential for catalysis and that it does not serve as the site of a protein-based free radical during catalysis. This is in agreement with previous kinetic data that showed the intervention of such a radical was highly unlikely (*37*). Nevertheless, although K_M for succinyl-CoA is essentially unchanged, k_{cat} and k_{cat}/K_M are lower by 580- and 380-fold, respectively, for the Tyr89Phe mutant, compared to wild-type, consistent with the loss of an interaction that stabilizes the transition state for the catalyzed reaction, rather than an effect on substrate binding. The kinetic deuterium isotope effect (Table 1) on conversion of succinyl-CoA into methylmalonyl-CoA was also measured and was found to be significantly greater in the mutant ($V_H/V_D = 5.2 \pm 0.8$) than in wild-type enzyme ($V_H/V_D = 3.4 \pm 0.5$), suggesting that the mutation has altered the energetics of catalysis so that the isotope-sensitive steps of hydrogen transfer (interconversion of EM and EM•, interconversion of ES and ES•, Figure 1) are contributing relatively more to overall rate limitation than in the wild-type (*39*). A more detailed analysis of the primary kinetic deuterium isotope effect on V_{max} alone is not yet possible, since the observed deuterium isotope contains contributions from at least two steps, hydrogen transfer from substrate to coenzyme (*10*), and hydrogen transfer from coenzyme to the product radical.

To analyze in more detail this apparent change in the energetics of the catalyzed reaction, we have studied the kinetics of release of tritium from AdoCbl during the reaction catalyzed by the Tyr89Phe methylmalonyl-CoA mutase and the partitioning of the released isotope between methylma-

lonyl-CoA and succinyl-CoA. In wild-type mutase tritium partitions identically, 75:25 in favor of succinyl-CoA over methylmalonyl-CoA, irrespective of which CoA ester is used to initiate the reaction, under conditions where the reverse reaction can be neglected (*37*). This indicates that, in wild-type mutase, the species EM· and ES· must be in rapid equilibrium with each other, as shown in Figure 5 (panels a and b), so that they are kinetically indistinguishable. This is not true for the Tyr89Phe mutant, where the partitioning ratio was found to differ depending on the CoA ester used as the substrate. When methylmalonyl-CoA was used as a substrate, the tritium released from AdoCbl was found to partition 60:40 in favor of succinyl-CoA, that is, rather less in favor of the product than with wild-type enzyme. When succinyl-CoA was used, the alteration in the partitioning ratio was also rather less in favor of the product, with only some 10% of the tritium released being found in methylmalonyl-CoA and 90% being found in succinyl-CoA. The dependence of the partitioning ratio upon the substrate used to initiate tritium release demonstrates that the species EM· and ES· are in this case clearly kinetically distinguishable: it appears that, as shown in Figure 5 (panels c and d), the rate of interconversion of the free radical species EM· and ES· has been sufficiently decreased by the loss of the interaction with the hydroxyl of tyrosine 89 that in each case the percentage of tritium found in the substrate is larger than in wild-type.

Further insight into the altered energetics in the Tyr89Phe mutant was obtained by measurement of the kinetic isotope effect for tritium release from AdoCbl. For wild-type enzyme, with methylmalonyl-CoA as substrate, the primary kinetic isotope effect was determined as $k_H/k_T = 4.9$ (*37*), which is considerably smaller than a normal primary tritium kinetic isotope effect, which lies in the range $k_H/k_T = 20-30$ (*39*). This suppressed effect was taken to mean that the energetics of the wild-type mutase are balanced, with steps other than hydrogen transfer (such as product release, breakage of the cobalt−carbon bond) contributing to overall rate limitation (*37*). In contrast, for the mutant enzyme, the tritium isotope effect, with methylmalonyl-CoA as substrate, was found to be $k_H/k_T = 30$. This full isotope effect clearly indicates that, in the Tyr89Phe mutant, not only the interconversion of the radical species EM· and ES· but also the hydrogen-transfer steps are much slower than those in the wild-type.

A qualitative free-energy profile representing all the kinetic data obtained in this study is shown in Figure 6b, where it is compared with the free-energy profile previously deduced for the wild-type enzyme (Figure 6a). The tritium effects are shown for clarity as effects on the transition state, although they actually affect the ground state. An important difference between the two profiles is that, for the mutant step 3, the interconversion of EM· and ES· is a significant step. This accounts for the different partitioning ratios arising from tritium release when different substrates are used. Step 3 (Figure 6b) is shown as comparable to steps 2 and 4, since all three are probably much slower than steps 1 and 5, as shown by the full tritium isotope effect found for release of tritium from AdoCbl with methylmalonyl-CoA as substrate and, yet, the primary kinetic deuterium isotope effect (which affects steps 2 and 4 only) is partly suppressed, as would be expected if step 3 is also slow. The equilibrium constant

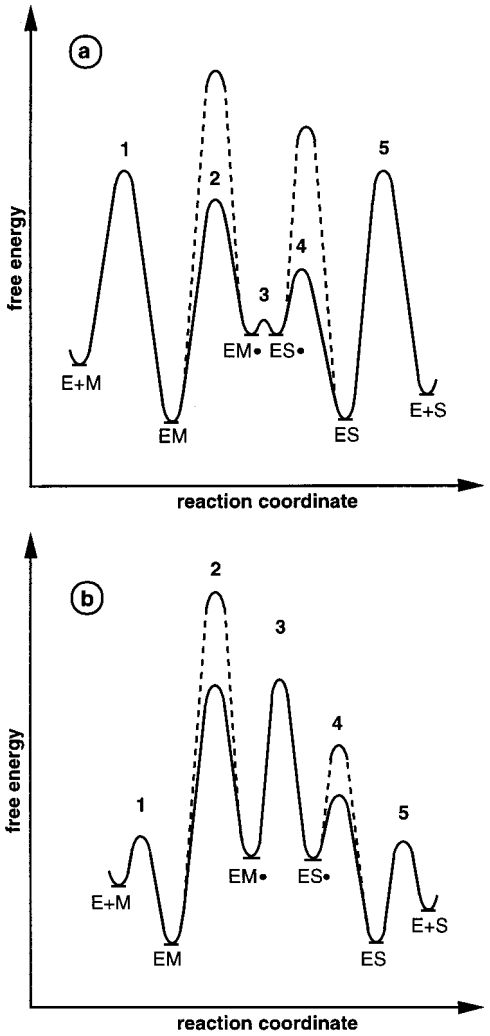

FIGURE 6: Qualitative free energy profile of the reaction catalyzed wild-type (a) and by the Tyr89Phe mutant of methylmalonyl-CoA mutase (b). Methylmalonyl-CoA (M), Succinyl-CoA (S), and their substrate-based radicals are depicted as EM· and ES·, respectively. In the absence of further quantitative data, the absolute free energy values are chosen arbitrarily. The plain line represents the energy profile for hydrogen, whereas the dashed line is a superimposed energy profile for tritium.

for the mutase-catalyzed reaction is 1:20 in favor of succinyl-CoA (*32*), and the profile is also drawn to reflect the fact that tritium release when succinyl-CoA is used as substrate is 4 times faster than when methylmalonyl-CoA is used (step 4 has a lower barrier than step 2). The energy minima of the bound substrates are set at the same level, an assumption which is supported by the crystal structure showing approximately equal electron density for both substrates. In the absence of further data, the radical intermediates EM· and ES· are arbitrarily set at the same level.

The X-ray crystal structure of wild-type mutase in the absence of substrate (*17*) shows that the aromatic ring of tyrosine 89 is stacked closely against the adenine ring of the AdoCbl. Comparison with structures of the mutase containing substrate or substrate analogues is hindered by the fact that in the latter complexes the adenosyl moiety has not been localized, but it appears that upon substrate binding, the side chain of tyrosine 89 is moved closer to the cobalamin, displacing the adenosyl group (*17*). The loss of the hydroxyl group (Figure 7B), which in the wild-type

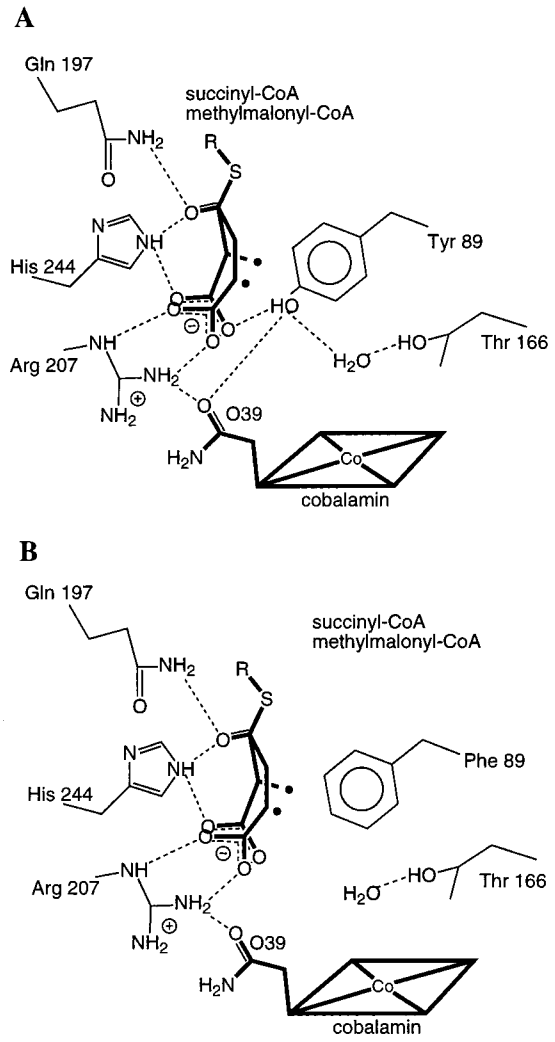

FIGURE 7: Schematic drawing of the active site of wild-type (A) and the Tyr89Phe mutant of methylmalonyl-CoA mutase (B). The two substrate-derived radicals are indicated by a dot (●).

(Figure 7A) appears to be involved in hydrogen-bonding interactions with substrate, a side chain of the corrin ring, and the protein (relayed via a water molecule), would be predicted to have little effect on initial substrate-induced cobalt−carbon bond cleavage. However, if this interaction served to anchor the adenosyl group and/or the substrate in an optimal conformation for hydrogen transfer, its loss in the mutant would be expected to slow steps 2 and 4, as is observed. In addition, however, it is clear that the interconversion of the radical intermediates EM· and ES· is significantly affected by the loss of this interaction. Both associative (see, e.g., ref *40*) and dissociative (*41*) mechanisms have been proposed for this interconversion, and the experiments in this paper do not distinguish between them. Apparently, differential stabilization of one or more transition states between EM· and ES· is achieved by specific hydrogen bonding to tyrosine 89. Taken together, these results furnish the first evidence that such specific effects are exerted by side chains at the active site of AdoCbl-dependent mutases.

ACKNOWLEDGMENT

We thank Professor Neil Marsh (University of Michigan, Ann Arbor, MI) for the kind gift of glutamate mutase. N.H.T. thanks the Studienstiftung des Deutschen Volkes for a graduate studentship.

REFERENCES

1. Eggerer, H., Overath, P., Lynen, F., and Stadtman, E. R. (1960) *J. Am. Chem. Soc. 82*, 2643−2644.
2. Sprecher, M., Clark, M. J., and Sprinson, D. B. (1966) *J. Biol. Chem. 241*, 872−877.
3. Banerjee, R. (1997) *Chem. Biol. 4*, 175−186.
4. Ludwig, M. L., and Matthews R. G. (1997) *Annu. Rev. Biochem. 66*, 269−313.
5. Thomä, N. H., and Leadlay, P. F. (1998) *Biochem. Soc. Trans.* (in press).
6. Zhao, Y., Such, P., and Rétey, J. (1992) *Angew. Chem., Int. Ed. Engl. 31*, 215−216.
7. Keep, N. H., Smith, G. A., Evans, M. C. W., Diakun, G. P., and Leadlay, P. F. (1993) *Biochem. J. 295*, 387−392.
8. Zhao, Y., Abend, A., Kunz, M., Such, P., and Rétey, J. (1994) *Eur. J. Biochem. 225*, 891−896.
9. Padmakumar, R., and Banerjee, R. (1995) *J. Biol. Chem. 270*, 9295−9300.
10. Padmakumar, R., Padmakumar, R., and Banerjee R. (1997) *Biochemistry 36*, 3713−371.
11. Erfle, J. D., Clark, J. M. J., Nystrom, R. F., and Johnson, B. C. (1964) *J. Biol. Chem. 239*, 1920−1924.
12. Rétey, J., and Arigoni, D. (1966) *Experientia 22*, 783−784.
13. Cardinale, G. J., and Abeles, R. H. (1967) *Biochim. Biophys. Acta 132*, 517−518.
14. Hay, B. P., and Finke, R. G. (1987) *J. Am. Chem. Soc. 109*, 8012−8018.
15. Pratt J. M.(1985) *Chem. Soc. Rev 14*, 161−170.
16. Mancia, F., Keep, N. H., Nakagawa, A., Leadlay, P. F., McSweeney, S., Rasmussen, B., Bösecke, P., Diat, O., and Evans, P. R. (1996) *Structure 4*, 339−350.
17. Mancia, F., and Evans, P. R. (1998) *Structure 6*, 711−720.
18. Drennan, C. L., Huang, S., Drummond, J. T., Matthews, R. G., and Ludwig, M. L. (1994) *Science 266*, 1669−1674.
19. Ludwig, M. L., Drennan, C. L., and Matthews, R. G. (1996) *Structure 4*, 505−512.
20. Rétey, J. (1990) *Angew. Chem., Int. Ed. Engl. 29*, 355−361.
21. Pedersen, J. Z., and Finazzi-Agrò, A. (1993) *FEBS Lett. 325*, 53−58.
22. Musah, R. A., and Goodin, D. B. (1997) *Biochemistry 36*, 11665−11674.
23. McKie, N., Keep, N. H., Patchett, M. L., and Leadlay, P. F. (1990) *Biochem. J. 269*, 293−298.
24. Marsh, E. N. G. (1995) *Biochemistry 34*, 7542−7547.
25. Simon, E. J., and Shemin, D. (1953) *J. Am. Chem. Soc. 75*, 2520.
26. Michenfelder, M., and Rétey, J. (1986) *Angew. Chem., Int. Ed. Engl. 25*, 366−367.
27. Higuchi, R., Krummel, B., and Saiki, R. K. (1988) *Nucleic Acids Res. 16*, 7351−7367.
28. Navaza, J. (1994) *Acta Crystallogr., Sect. A 43*, 489−501.
29. Murshudov G. N., Vagin A. A., and Dodson E. J. (1997) *Acta Crystallogr., Sect. D 53*, 240−255.
30. Jones, T. A., Zou, J. Y., Cowan, S. W., and Kjeldgaard M. (1991) *Acta Crystallogr., Sect. A 43*, 489−501.
31. Keep, N. H. (1992) Ph.D. Thesis, University of Cambridge.
32. Kellermeyer, R. W., Allen, S. H. G., Stjernholm, R., and Wood, H. G. (1964) *J. Biol. Chem. 239*, 2562−2569.
33. Zagalak, B., Rétey, J., and Sund, H. (1974) *Eur. J. Biochem. 44*, 529−535.
34. Cornish Bowden A. (1995) *Fundamentals of Enzyme Kinetics*, Portland Press, London.
35. Evans, P. R., and Mancia, F. (1998) in *Vitamin B_{12} and B_{12}-proteins* (Kräutler, B., Arigoni, D., and Golding, B. T., Eds.) pp 217−226, Wiley-VCH, Mannheim.

36. Wölfle, K., Michenfelder, M., König, A., Hull, W. E., and Rétey, J. (1986) *Eur. J. Biochem. 156*, 545−554.
37. Meier, T. W., Thomä, N. H., and Leadlay, P. F. (1996) *Biochemistry 35*, 11791−11796.
38. Gaudemer, A., Zylber, J., Zylber, N., Baran-Marszac, M., Hull, W. E., Fountoulakis, M., König, A., Wölfle, K., and Rétey, J. (1981) *Eur. J. Biochem. 119*, 279−285.
39. Walsh, C. T. (1979) *Enzymatic reaction mechanisms*, Wiley & Sons, San Francisco.
40. Halpern, J. (1985) *Science 227*, 869−875.
41. Beatrix, B., Zelder, O., Kroll, F., Örlygsson, G., Golding, B. T., and Buckel, W. (1995) *Angew. Chem., Int. Ed. Engl. 34*, 2398−2401.

BI981375O